Supporting information

Photoacoustic Imaging Quantifies Drug Release from Nanocarriers via Redox Chemistry of Dye-Labeled Cargo

Ananthakrishnan Soundaram Jeevarathinam[a]‡, Jeanne E. Lemaster[a]‡, Fang Chen#[a,c], Eric Zhao[a], and Jesse V. Jokerst[a,b,c]*

*Corresponding Author

E-mail: jjokerst@ucsd.edu

[a]. Department of NanoEngineering, University of California San Diego, 9500 Gilman Drive, La Jolla, CA, 92093, USA
[b]. Materials Science and Engineering Program, University of California, San Diego, 9500 Gilman Dr., La Jolla, CA 92093, USA.
[c]. Department of Radiology, University of California, San Diego, 9500 Gilman Dr., La Jolla, CA 92093, USA.

‡ *These authors contributed equally to this work.*
# Current Address: Stanford University

Synthesis of key intermediates.

PTX-COOH was synthesized according to the previously reported procedures.[1] In a typical synthesis of (PTX-COOH), Paclitaxel (M.W. 853.90 g mol^{-1}; 100.0 mg; $1.17x10^{-4}$ mol), 4-dimethylaminopyridine (M.W., 122.16 g mol^{-1}; 23.6 mg; $1.93x10^{-4}$ mol) and of succinic anhydride (M.W., 100.07 g mol^{-1}; 40.9 mg; $4.09x10^{-4}$ mol) were placed under nitrogen in a round bottomed flask. Then, dry pyridine (3 mL) was added to dissolve the above reactants and the solution was stirred for 3 hours at room temperature. After 3 hours, anhydrous dichloromethane (12 ml) was added. The combined solution was washed with 1 M HCl (3 x 12 ml) and with deionized water (3 x 12 ml). The aqueous phase was again washed with dichloromethane (10 ml). The combined organic phase was evaporated under vacuum in a rotary evaporator. The resulting crude 2'-succinimidyl paclitaxel (II) (PTX-COOH) was used without further purification. The product was isolated as colorless powder in 65 % isolated yield and purity of the sample was found to be 99.6%. MS (LC-ESI) m/z $[M+H]^+$ calcd for C_{51} H_{56} NO_{17} 954.08; found 954.08 (LC-MS data is shown in Figure S1 & S2).

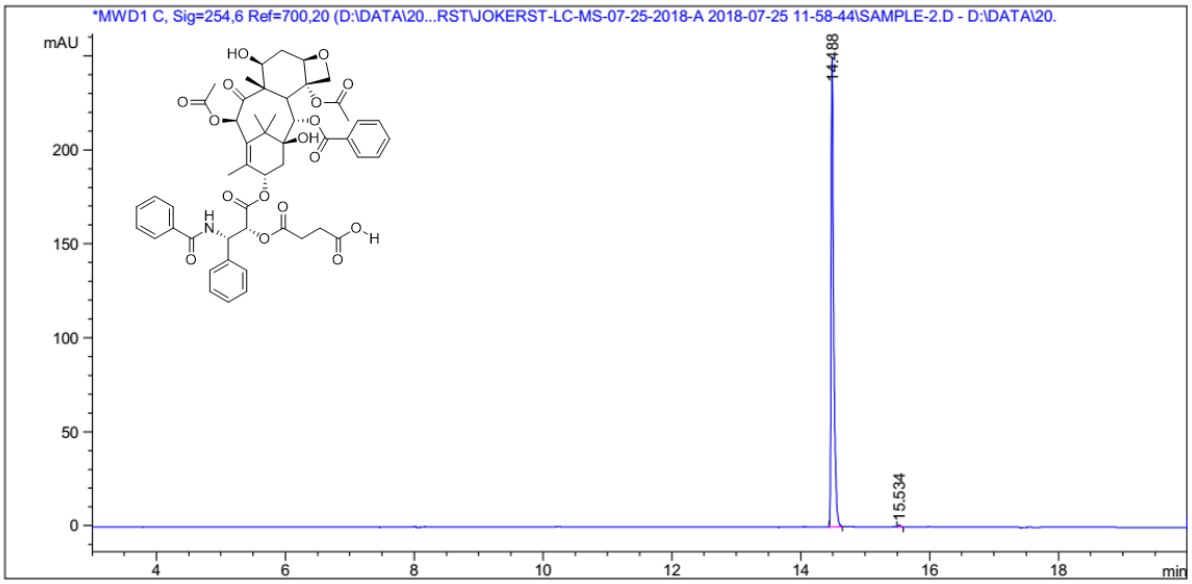

Figure S1. Liquid chromatography trace from the LC-MS analysis of (II). Retention time, 14.48 min with 99.6 % purity

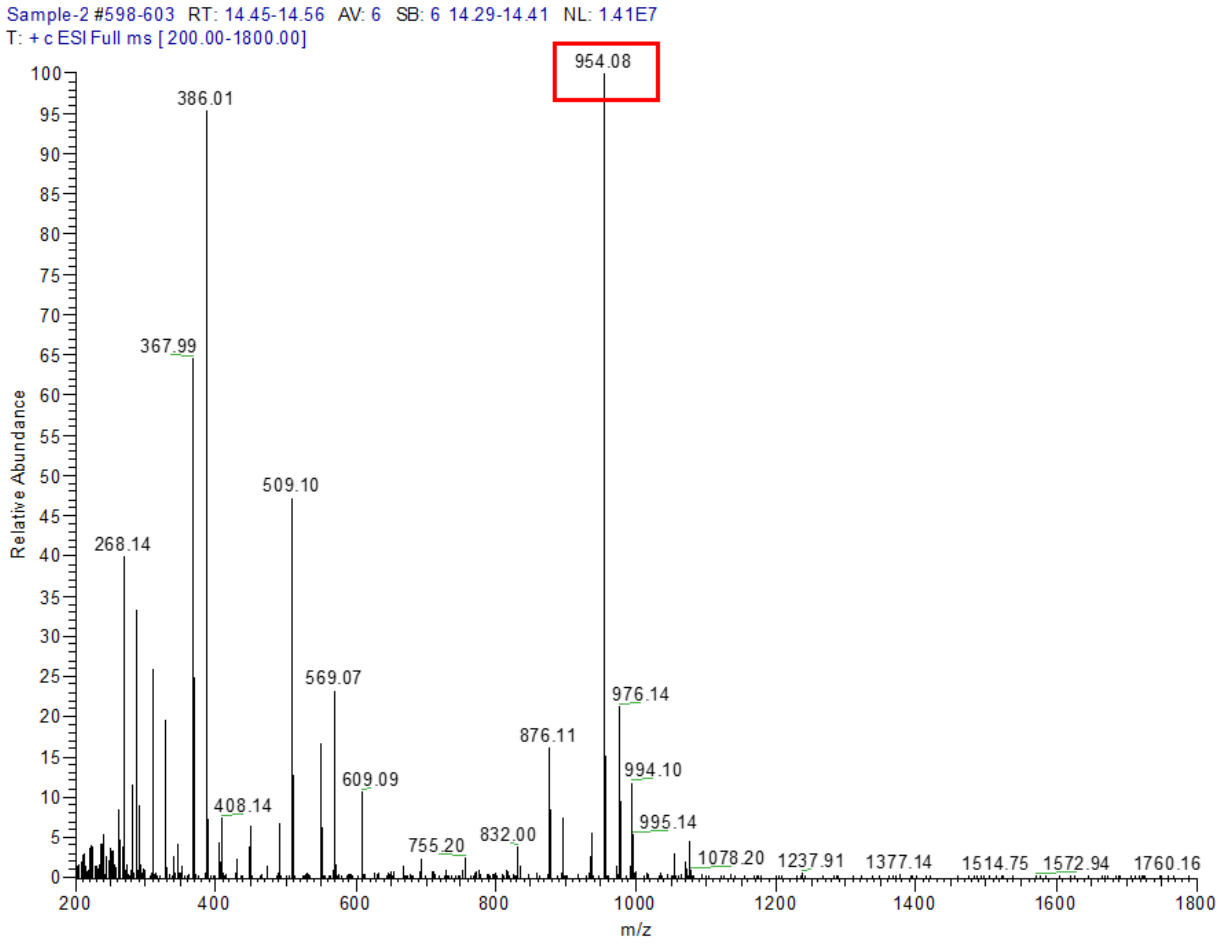

Figure S2. Mass spectrum of the sample of (II) from the LC-MS analysis corresponding to **Figure S1**

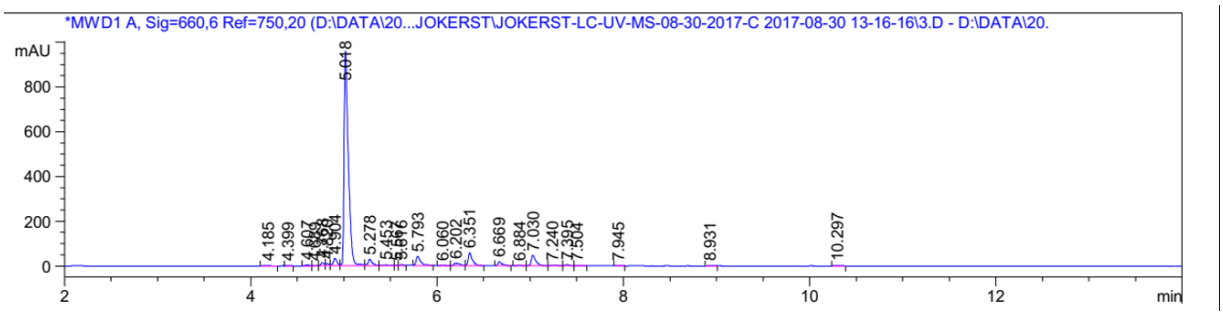

Figure S3. Liquid chromatography trace from the LC-MS analysis of dye (III). Retention time, 5.018 min with 74.6 % purity

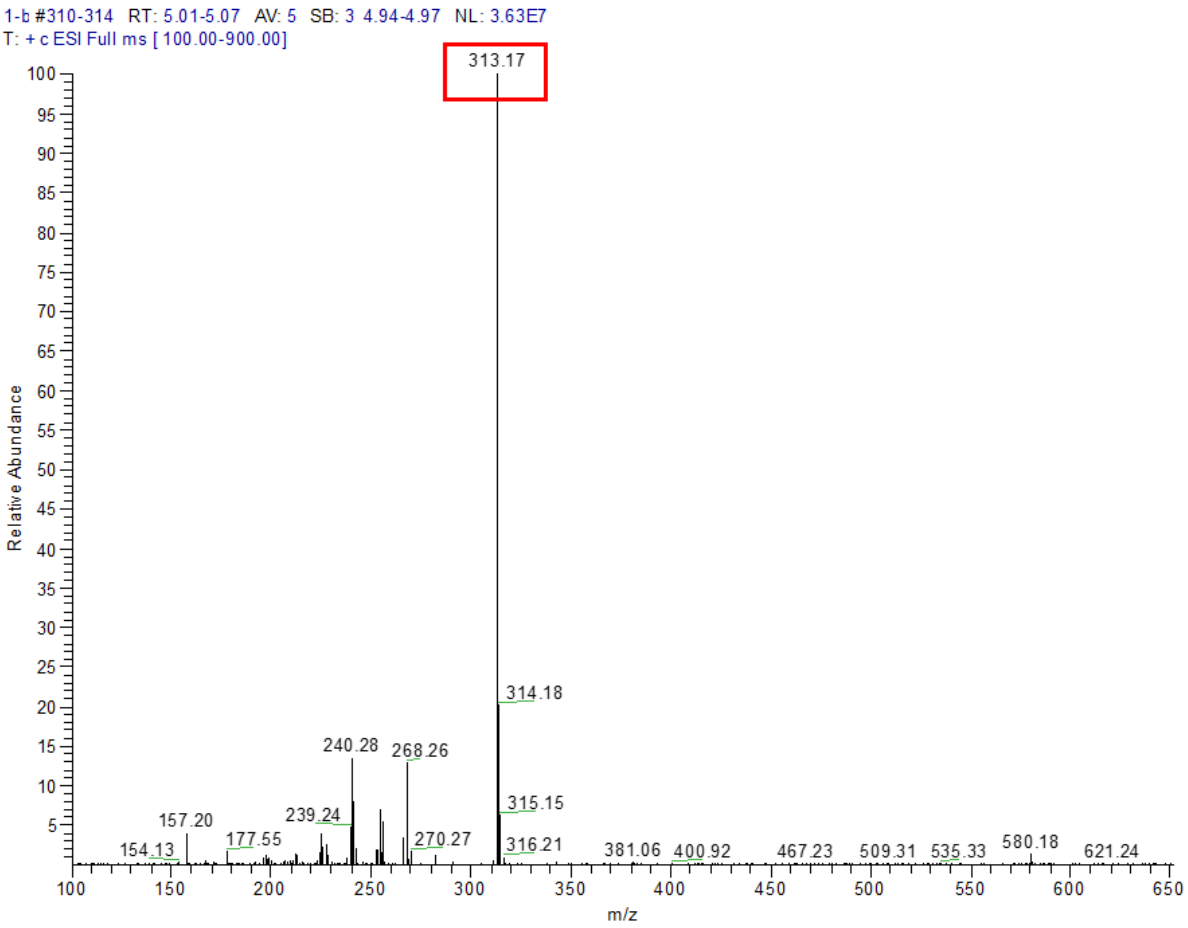

Figure S4. Mass spectrum from LC-MS analysis of dye (III) corresponding to **Figure S3.**

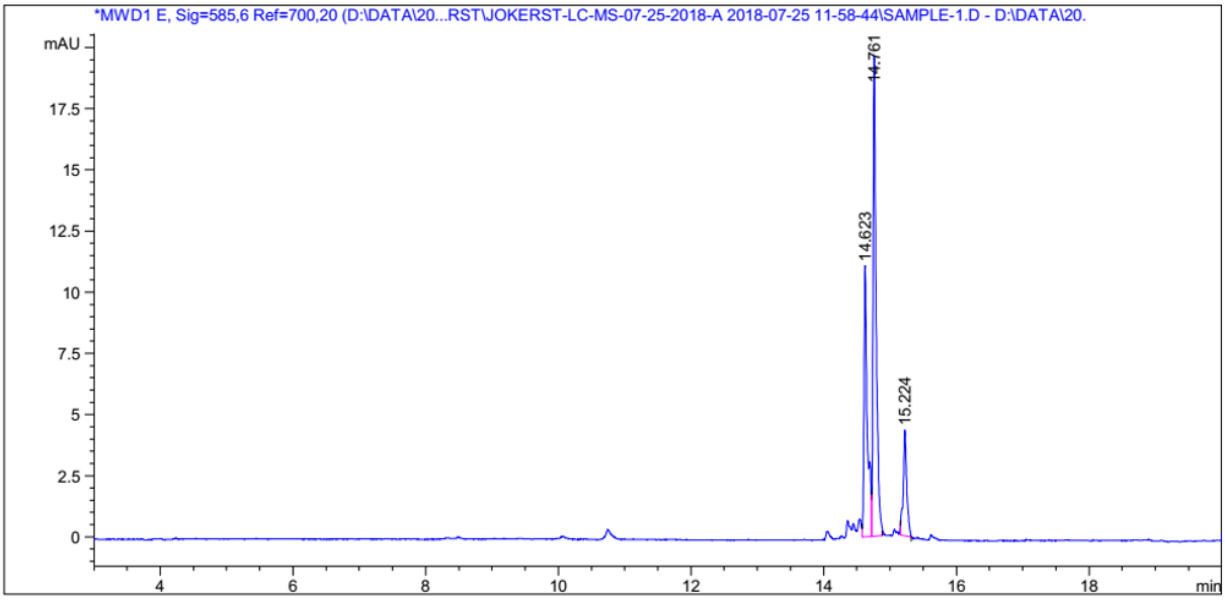

Figure S5. Liquid chromatogram of PTX-MB from LC-MS analysis of crude sample of PTX-MB obtained from reaction mixture corresponding to Figure 3S. Retention time is 14.78 min with an overall yield of 53.8 %.

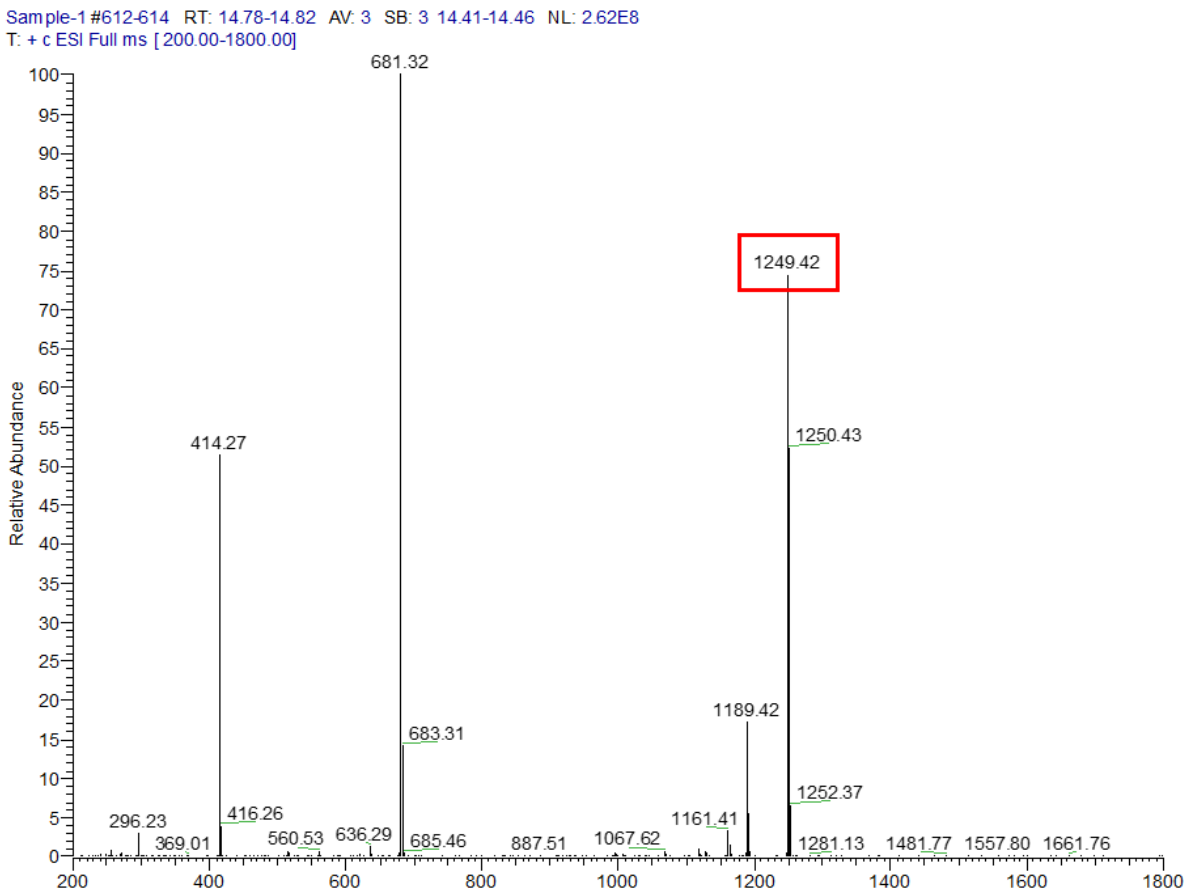

Figure S6. Mass spectrum from the LC-MS analysis of crude sample of PTX-MB. The mass spectrum corresponds to the peak with retention time of 14.78 min in **Figure 5S**.

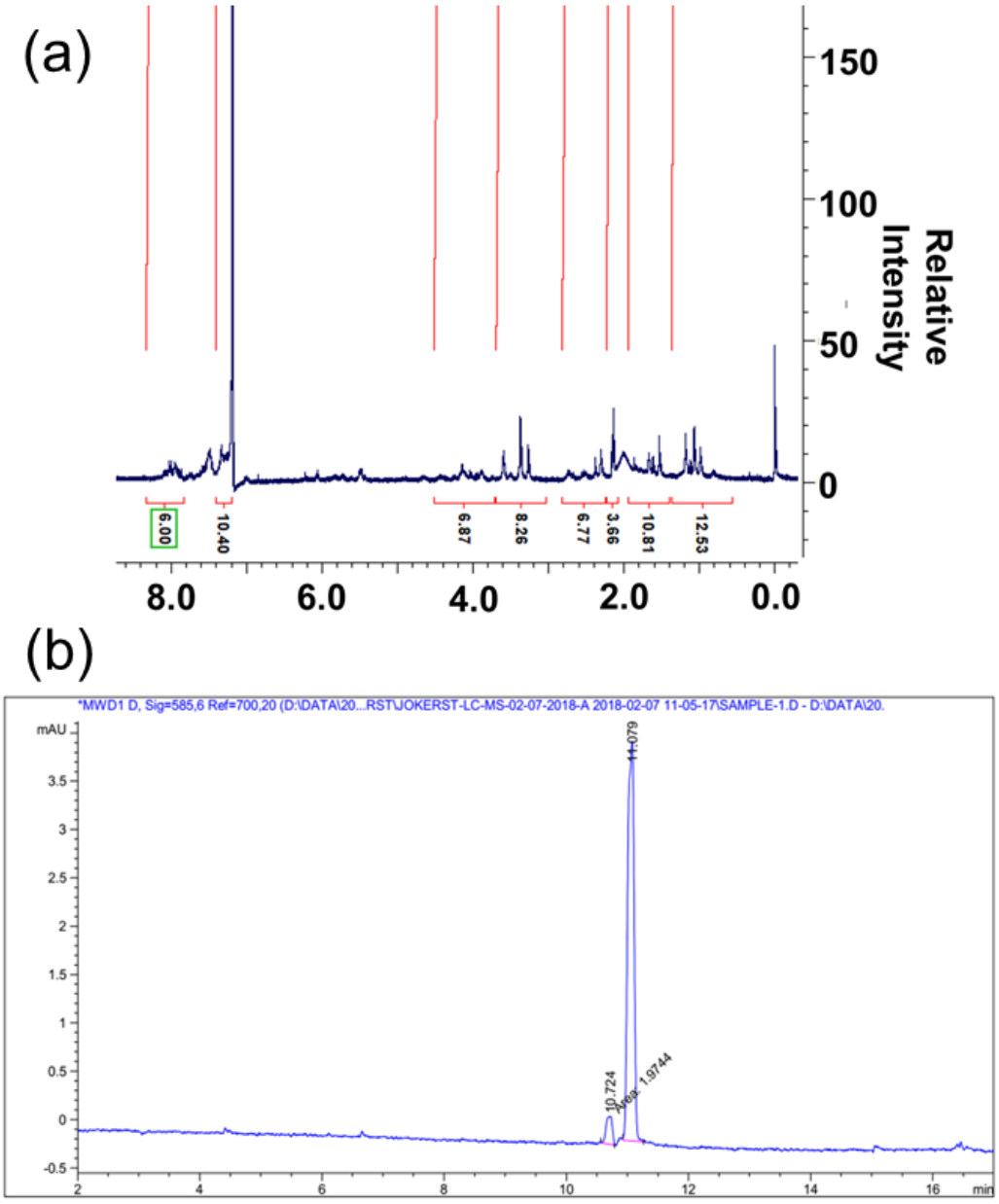

Figure S7. (a) NMR spectrum of PTX-MB purified by HPLC . (b) Liquid chromatogram of PTX-MB after purification by reverse phase HPLC with a mobile phase gradient of 30 -60 % water in acetonitrile with 0.01 %v/v of trifluoroacetic acid. Retention time is 11.0 min with purity of 93.6%. Compound was isolated as trifluoroacetate salt.

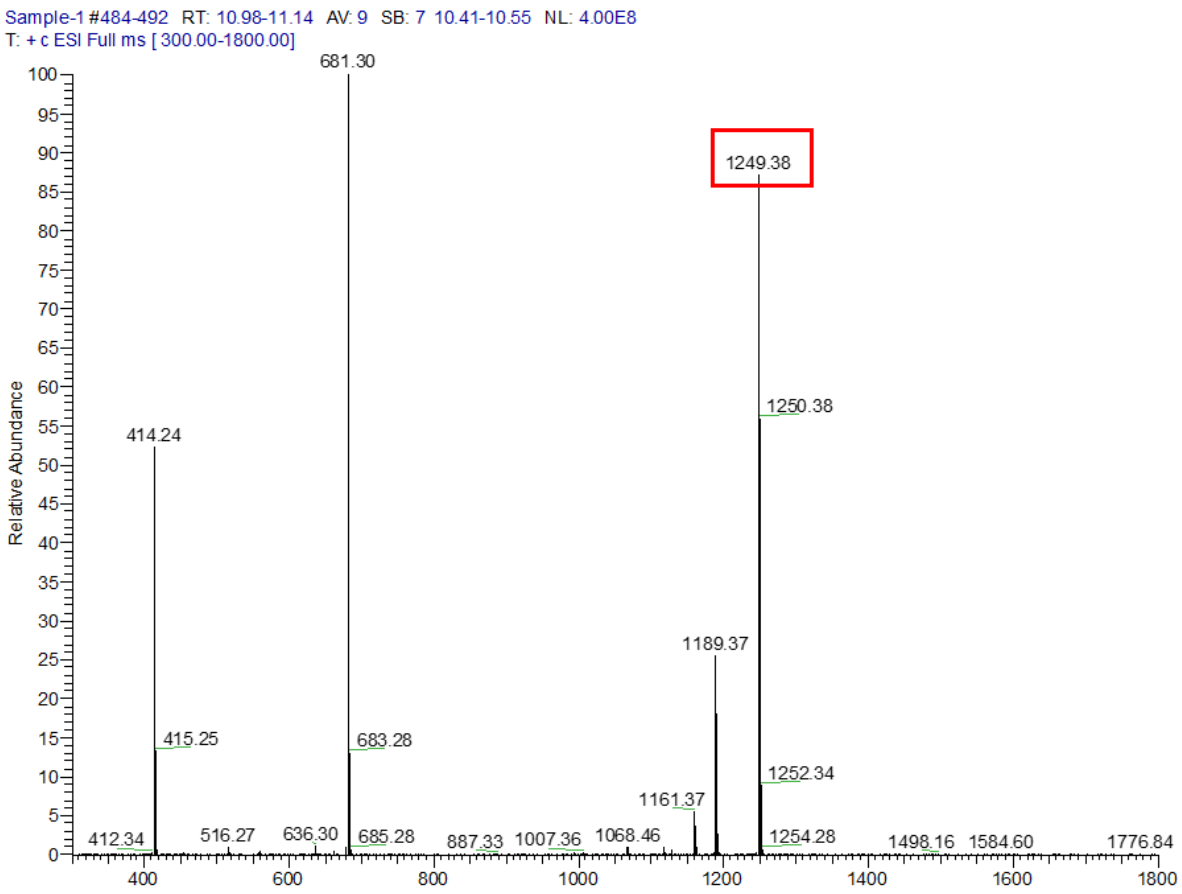

Figure S8. Mass spectrum of PTX-MB after purification by reverse phase HPLC. The spectrum corresponds to the peak with retention time of 11.0 min in **Figure 7S.**

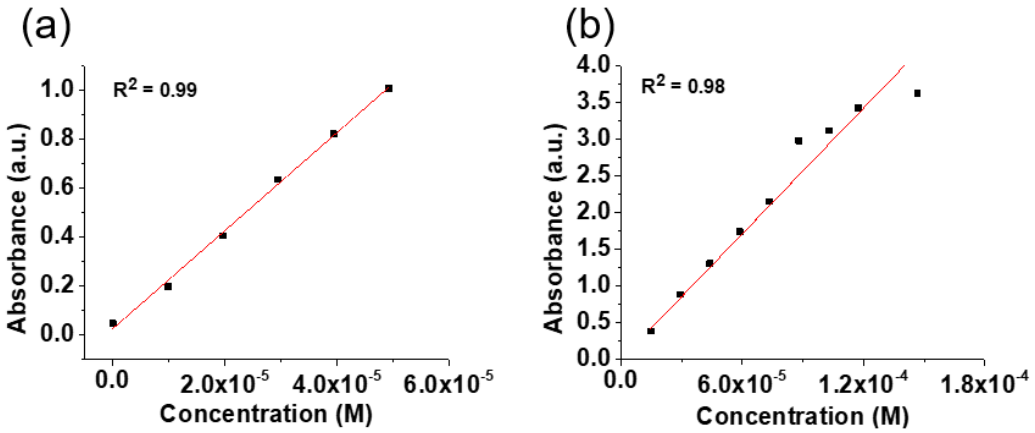

Figure S9. (a) Calibration of absorbance of PTX-MB with its concentration in PBS medium containing 20 % v/v normal mouse serum.

Figure S10. (a) Absorbance of supernatants collected during the drug release study of PLGA NPs loaded with PTX-LMB in PBS with 20 % mouse serum at 0, 1, 3, 6, 12, 24,48, 72, 96, and 120 hours. (b) photograph of the aliquots collected corresponding to the absorbance in (a). (c) the particles isolated from each aliquots were dispersed in 1% agarose to avoid precipitation (leading to small variations in photoacoustic signal) and 3D image of the dispersions were acquired after the allowing the dispersion to solidify. (c) shows that the photoacoustic intensity of the isolated particles did not follow a specific trend. This is in contrast to the photoacoustic signal of the supernatants of the aliquots.

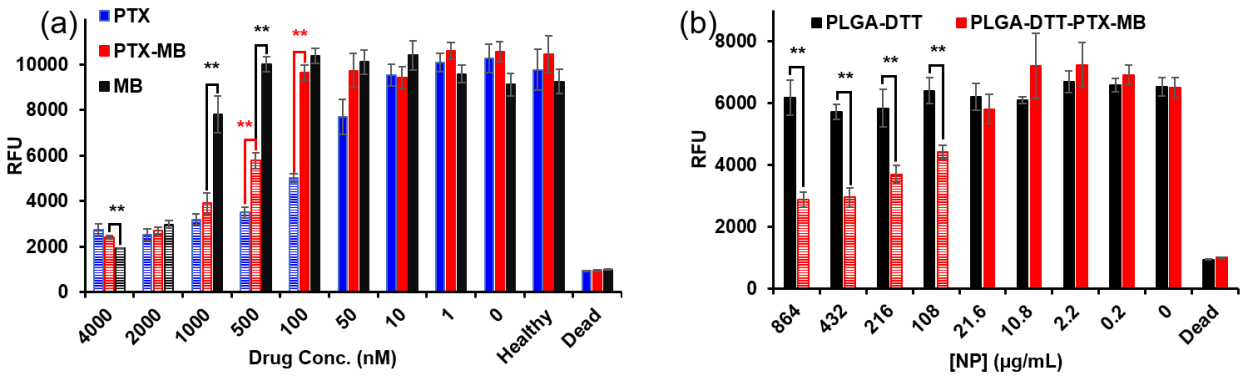

Figure S11. (a) Dose-response curve of the drugs. The half maximal inhibitory concentration (IC50) of PTX, PTX-MB, and MB are 68, 447, and 1281 nM respectively. Striped columns have a $p < 0.001$ compared to the group without drug (0 nM). S: $p<0.001$ (two tail, homoscedastic student t-test). (b) Dose-response curve of the PLGA-DTT-PTX-MB. The half maximal inhibitory concentration (IC50) of PLGA-DTT-PTX-MB is 78 µg/mL or 362 nM PTX-MB after one-hour release. Striped columns have a $p < 0.001$ compared to the group without nanoparticles (0 µg/mL). S: $p<0.001$ (two tail, homoscedastic student t-test).

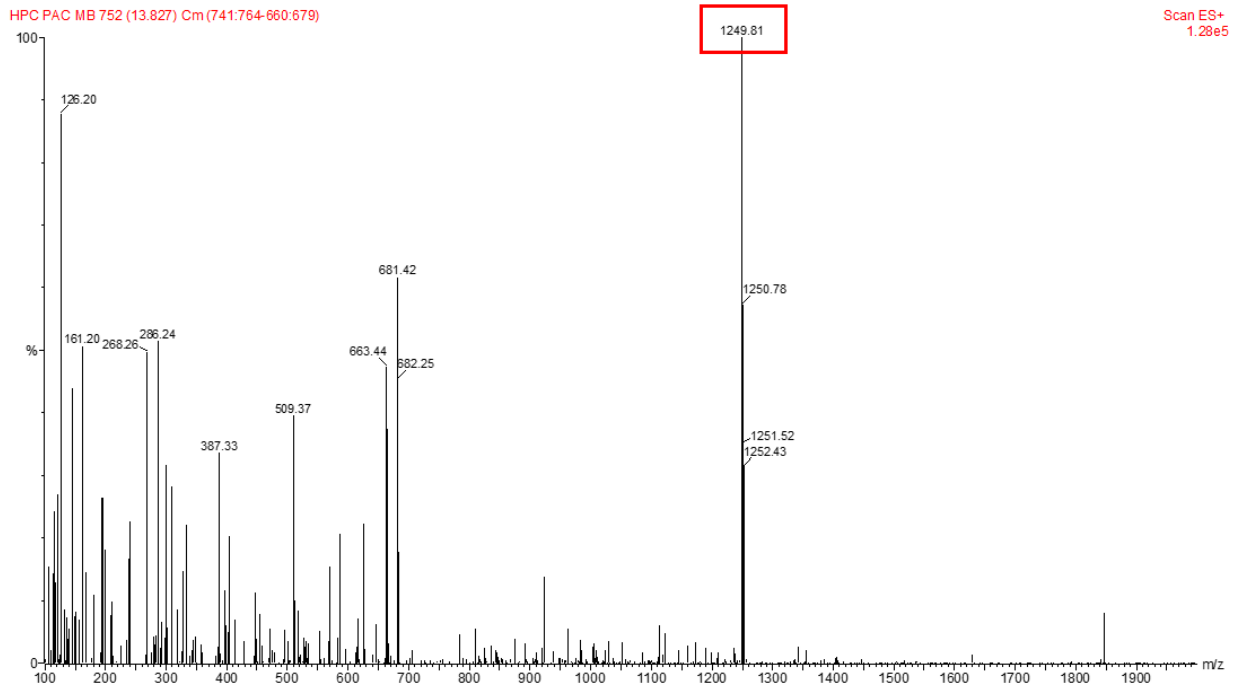

Figure S12. ESI-mass spectrum of PTX-MB extracted form the supernatant of the aliquot collected from drug release study at 120 h. No detectable amounts of DTT was found in the aliquot.

Time points (h)	Experimental set 1	Experimental set 2	Experimental set 3	Control set
0	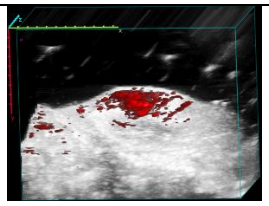	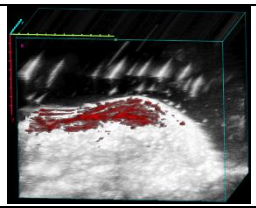	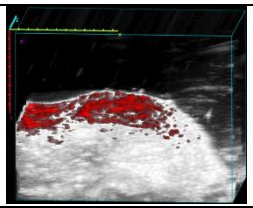	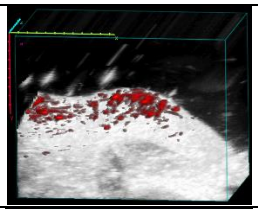
2	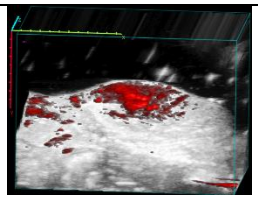	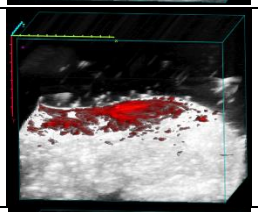	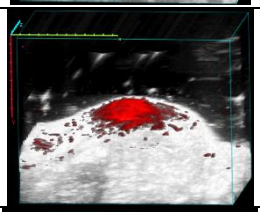	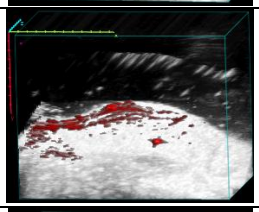
4	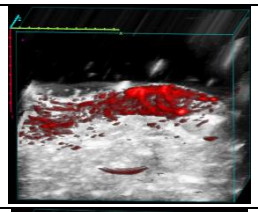	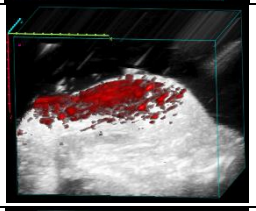	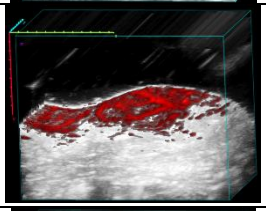	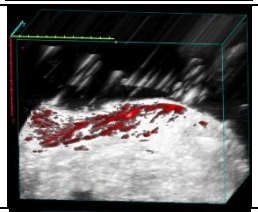
6	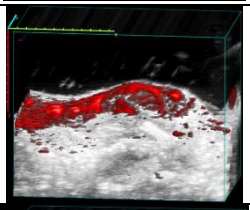	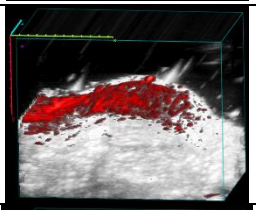	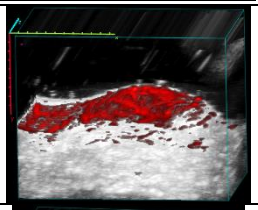	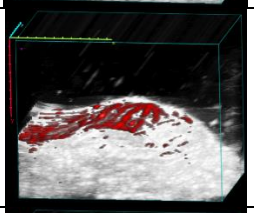
8	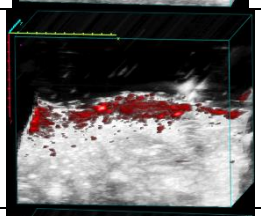	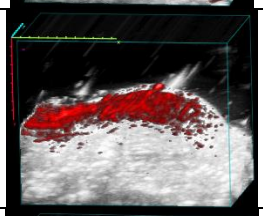	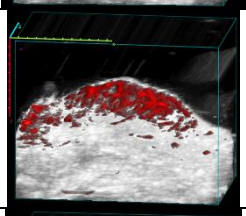	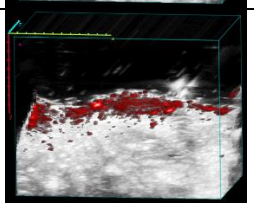
10	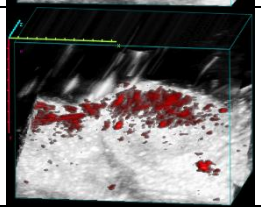	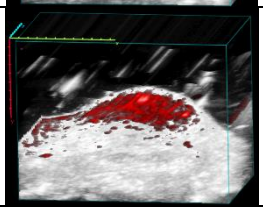	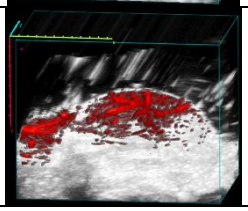	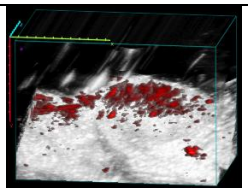

Figure S13. Photoacoustic 3D images of experimental and control sets of mice at different time points obtained from the in-vivo drug release studies.

References

1. Gao, Y.; Kuang, Y.; Guo, Z.-F.; Guo, Z.; Krauss, I. J.; Xu, B., Enzyme-Instructed Molecular Self-assembly Confers Nanofibers and a Supramolecular Hydrogel of Taxol Derivative. *Journal of the American Chemical Society* **2009,** *131* (38), 13576-13577.
2. Felgentraeger, A.; Maisch, T.; Dobler, D.; Spaeth, A., Hydrogen bond acceptors and additional cationic charges in methylene blue derivatives: photophysics and antimicrobial efficiency. *BioMed Res. Int.* **2013**, 482167, 12 pp.
3. Fonte, P.; Soares, S.; Costa, A.; Andrade, J. C.; Seabra, V.; Reis, S.; Sarmento, B., Effect of cryoprotectants on the porosity and stability of insulin-loaded PLGA nanoparticles after freeze-drying. *Biomatter* **2012,** *2* (4), 329-339.
4. Holzer, M.; Vogel, V.; Mäntele, W.; Schwartz, D.; Haase, W.; Langer, K., Physico-chemical characterisation of PLGA nanoparticles after freeze-drying and storage. *European Journal of Pharmaceutics and Biopharmaceutics* **2009,** *72* (2), 428-437.
5. Zaias, J.; Mineau, M.; Cray, C.; Yoon, D.; Altman, N. H., Reference values for serum proteins of common laboratory rodent strains. *J Am Assoc Lab Anim Sci* **2009,** *48* (4), 387-390.